

## Supporting Information: Zero valent iron core – iron oxide shell nanoparticles as small magnetic particle imaging tracers

Lucy Gloag,\* Milad Mehdipour, Marina Ulanova, Kevin Mariandry, Muhammad Azrhy Nichol, Daniela J. Hernández-Castillo, Jeff Gaudet, Ruirui Qiao, Ji Zhang, Melanie Nelson, Benjamin Thierry, Mayra A. Alvarez-Lemus, Thiam T. Tan, J. Justin Gooding, Nady Braidy, Perminder S. Sachdev, Richard D. Tilley\*

### Experimental:

Chemicals used: Ferrocene (98%), aluminium chloride (99%), benzene (anhydrous, 99.8%), aluminium powder (complexometric, >91%), potassium hexafluorophosphate (98%), lithium aluminium chloride (95%), mesitylene (98%) and oleylamine (OLA, >98% primary amine) were purchased from Sigma Aldrich. THF (99.9%) was purchased from ChemSolute. The RAFT agent, 2-(bis((dimethoxyphosphoryl)methyl)amino)ethyl 2-(((butylthio)carbonothioyl)thio)propanoate, was purchased from Boron Molecular. U251 glioma and HeLa cell lines were purchased from ATCC. Roswell Park Memorial Institute (RPMI) media 1640, 0.25% Trypsin-EDTA (1X) and GlutaMAX were purchased from Gibco (Auckland, NZ). The antibiotic antimycotic solution was purchased from Sigma Aldrich (Castle Hill, Australia). All chemicals were used without further purification.

Synthesis of 11 nm Fe(0) nanoparticles: Iron seeds were first synthesized by reducing  $\text{Fe}(\text{C}_5\text{H}_5)(\text{C}_6\text{H}_7)$  iron precursor<sup>1</sup> (0.3 g, 0.75 mmol) dissolved in 6 mL mesitylene and oleylamine (1.5 mL, 2.3 mmol) in a Fischer-Porter bottle filled with hydrogen gas (3 bar) at 130 °C for 72 h. To ensure all reagents were air-free, all liquids were degassed under vacuum and argon prior to use. Following reaction, the solution was cooled and transferred to a glove box. 2 mL crude iron seed solution was added to a mixture of  $\text{Fe}(\text{C}_5\text{H}_5)(\text{C}_6\text{H}_7)$  iron precursor (0.3 g, 0.75 mmol), 6 mL mesitylene and oleylamine (0.5 mL, 0.75 mmol). The solution was transferred to a Fischer Porter bottle, filled with 3 bar hydrogen gas and heated at 130 °C for 72 h. This process was repeated one more time before exposing to air and purification.<sup>2</sup> To purify, the nanoparticles were first conjugated to oleic acid by stirring a 2:1 crude solution:oleic acid mixture at 70 °C for 2 h. The brown precipitate was separated by centrifugation at 4000 rpm for 10 minutes with 1:1 crude solution:ethanol. The purification process was repeated two more times and the precipitate was redispersed in toluene for further functionalization.

Synthesis of 14 nm Fe(0) nanoparticles: The synthesis of 14 nm Fe(0) nanoparticles was identical to the synthesis of 11 nm Fe(0) nanoparticles with one further iteration using the 11 nm Fe(0) nanoparticles as seeds.

Synthesis of 14 nm Fe oxide nanoparticles: The nanoparticles were synthesized following a commonly adopted method.[3,4] Two solutions, (i)  $\text{FeCl}_3$  (5.406 g, Aldrich, 99%) in 20 mL deionized (DI) water, and (ii)  $\text{FeCl}_2$  (1.988 g, Aldrich, 98%) in 5 mL of HCl (2 M), were added to 100 mL DI water under vigorous stirring. Then, 120 mL ammonia solution (2 M) was added and left to stir for 5 minutes. The black precipitate was purified by centrifugation at 3500 rpm for 20 minutes and redispersed in MilliQ water. The same purification process was repeated 4 additional times and the resulting precipitate was redispersed in MilliQ water.

Synthesis of brush PEG polymer: The RAFT CTA 2-(bis((dimethoxyphosphoryl)methyl)amino)ethyl 2-(((butylthio)carbonothioyl)thio)propanoate (28.4 mg, 0.06 mmol), poly(ethylene glycol) methyl ether acrylate (POEGA) (0.5 g, 3 mmol), AIBN (1 mg, 0.006 mmol) were dissolved in 2 mL 1,4-dioxane in a septa-sealed vial. The solution was degassed by sparging with  $\text{N}_2$  for 30 min and the reaction mixture was then stirred at 70 °C. The reaction was quenched after 5 h via rapid cooling and exposure to oxygen. Subsequently, the polymer was precipitated three times in a mixture of diethyl ether and petroleum spirit (B.R. 40 – 60 °C) (1:1 v/v) to remove the small molecules.

0.5 g (0.5 mmol) of bisphosphonate-terminated brush PEG was dissolved in 3 mL of anhydrous dichloromethane in a glass vial with a magnetic stirrer bar, and sealed with a septum. The solution was stirred at 0 °C under nitrogen flow and a solution of trimethylsilyl bromide (TMSBr, 147.5  $\mu\text{L}$ , 1 mmol) in 2 mL of DCM was added drop-wisely. The reaction mixture was stirred for 24 h at room temperature. At the end of the reaction, the large excess of bromosilane and DCM were removed by evaporation under low pressure. After total elimination of bromosilane, methanol (5 mL) was added to the flask and the stirring was continued for 24 h at room temperature. Then the final product deprotected brush PEG polymer was precipitated into a large quantity of petroleum ether (B.P. 40 – 60 °C) and washed with a 1:1 (v: v) mixture of petroleum ether and diethyl ether.

**Polymer coating:** A solution of 100 mg  $\text{mL}^{-1}$  brush PEG polymer in dichloromethane was added dropwise to a stirring solution of 10  $\text{mg}_{\text{Fe}} \text{mL}^{-1}$  nanoparticles in dichloromethane heated to 40 °C to give an overall 10:1 polymer:Fe ratio.<sup>3</sup> The mixture was stirred for 24 h, before cooling and purification. The nanoparticles were precipitated with petroleum benzene at 14000 rpm for 15 minutes. The nanoparticles were redispersed in MilliQ water and purified two more times. The nanoparticles were redispersed in MilliQ water and filtered through 0.45  $\mu\text{m}$  filters (Millipore Millex-HV, polyvinylidene fluoride membrane) to remove aggregates.

**Characterization:** TEM grids were prepared by drop casting a dilute solution of nanoparticles in toluene onto a carbon coated copper grid. Low resolution TEM images were obtained on a Phillips CM200 TEM. High resolution TEM images were obtained on a JEOL F200 field emission TEM. Fourier transform infrared (FTIR) spectroscopic analysis was performed on a Thermo Nicolet iS 5 FTIR spectrometer by accumulating a minimum of 16 scans and selecting a resolution of 2  $\text{cm}^{-1}$ . Dynamic light scattering measurements were taken on a Malvern Instruments Zetasizer instrument.

**Magnetic measurements:** Magnetization measurements were performed on a Quantum Design MPMS XL magnetometer. 0.2 mL nanoparticles in  $\text{CHCl}_3$  (5  $\text{mg mL}^{-1}$ , determined by ICP-MS) was deposited into a straw, the solvent was evaporated and the straw was sealed. The sample was placed in the centre of two magnetic flux sensors. Hysteresis loops were collected at room temperature between -6 to 6 kOe.

**Cell culture:** HeLa cervical cells and U251 glioma cells were cultured separately in Roswell Park Memorial Institute (RPMI, Gibco, Life Technologies Corporation, Auckland, NZ) medium supplemented with 10% fetal bovine serum (Sigma-Aldrich, Castle Hill, Australia), 1% antibiotic antimycotic solution (Sigma-Aldrich, Castle Hill, Australia), and 1% GlutaMAX™-1 (Gibco, Life Technologies Corporation, Auckland, NZ). Cells were maintained at 37°C in a humidified atmosphere containing 95% air/5%  $\text{CO}_2$ . Cells were seeded into 24-well tissue culture plate and allowed to reach 100% confluency or to a density of  $1 \times 10^5$  cells 24 hours prior to experimentation.

**Nanoparticle treatment and Trypan Blue test of cell viability:** Cells were treated in triplicate using the above described NPs with concentrations ranging between 0.05 – 100  $\mu\text{g}_{\text{Fe}} \text{mL}^{-1}$ , determined by ICP-MS. Following 24h incubation with selected concentrations of NPs, the trypan blue exclusion test was used to determine cellular viability. Briefly, cells were trypsinized and resuspended in culture media. 10 $\mu\text{l}$  of cells was incubated with trypan blue in a 1:1 dilution and used for counting the ratio of alive/dead cells, using a hemocytometer via an optical microscope. Blue-stained cells were counted as non-viable and unstained cells as viable.

**Magnetic particle imaging:** A phantom containing nanoparticle tracer solutions of five different concentrations, measured by ICP-MS was imaged with MPI on a MOMENTUM MPI system (Magnetic Insight Inc., CA, USA). The imager produces a 6 T/m x 6 T/m Field Free Line selection field, a 45 kHz drive field, and uses x-space MPI reconstruction. Projection images were acquired (FOV: 12 cm x 6 cm, 4 min total acquisition and reconstruction time), as well as tomographic images (FOV: 12 cm x 6 cm x 6 cm, 45 min total acquisition and reconstruction time). At each concentration a point source (1  $\mu\text{L}$ ) phantom was imaged and the maximum signal measured. Fiducials containing ferucarbotran nanoparticles (VivoTrax, Magnetic Insight Inc) were also prepared and analyzed in a similar fashion

to provide a standard to compare too. A linear regression model from the peak MPI signal at each concentration was used to assess the peak MPI signal per  $\mu\text{g}$  of Fe.

A particle resolution was calculated by measuring the plot profile of the undiluted point source phantoms. The point-spread function of the signal was approximated from the measured full-width, half maximum distance of the signal subtracted by the width of the point sources.

Imaging was performed with the VivoQuant software (inviCRO, MA, USA).

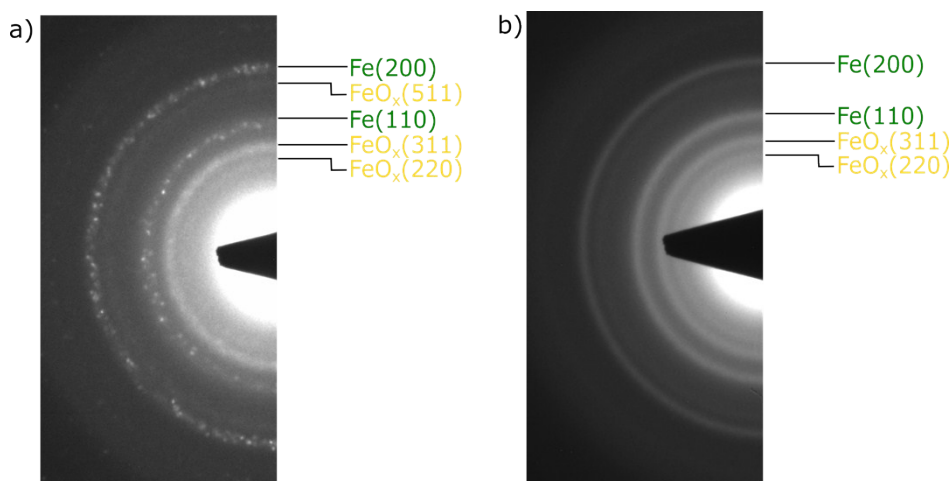


**Figure S1:** Selected area electron diffraction patterns for the zero valent iron core – iron oxide shell nanoparticles with a) 11 nm diameters (from Figure 1a) and b) 14 nm diameters (from Figure 1b). Rings are indexed to body centered cubic iron (green labels) and spinel-type iron oxide (magnetite or maghemite, yellow labels).

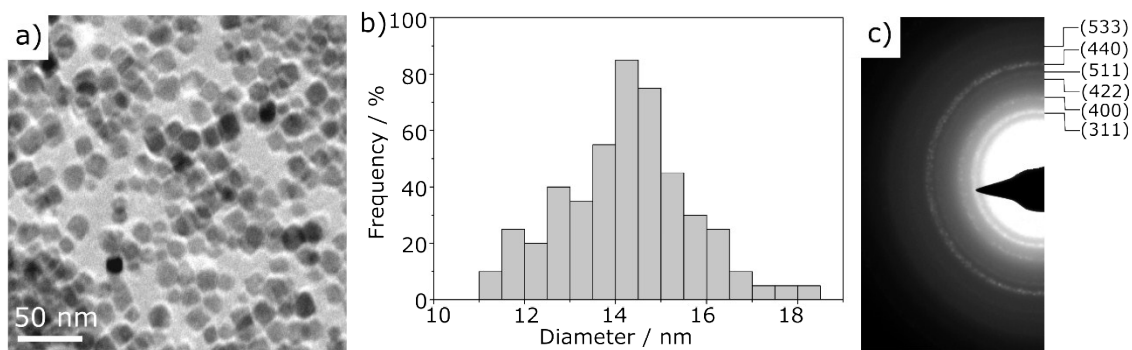


**Figure S2:** a) Low resolution TEM and b) corresponding histogram of the size distribution of 14 nm iron oxide nanoparticles. c) Selected area electron diffraction pattern of the nanoparticles in (a), indexed to the inverse spinel crystal structure of magnetite.

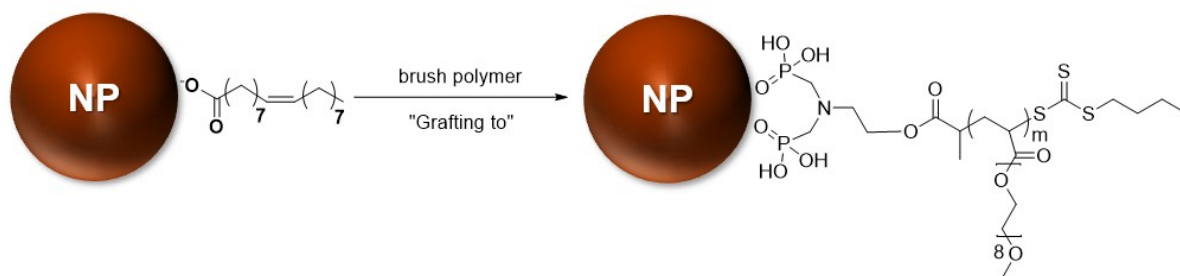


**Figure S3:** Scheme showing the ligand exchange of oleic acid with the multi-phosphonate brush PEG polymer.

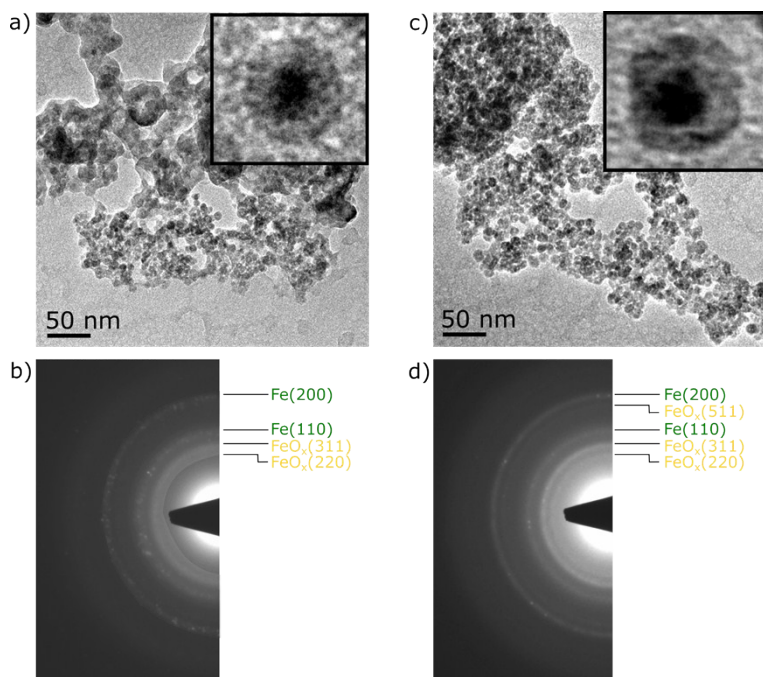


**Figure S4:** TEM characterization of the polymer coated nanoparticles after 8 weeks in aqueous media. a) TEM image of the 11 nm polymer coated nanoparticles with high magnification image showing the dark contrast zero valent iron core and light contrast iron oxide shell. b) SAED of the nanoparticles in (a) indexed to zero valent iron and iron oxide (magnetite or maghemite) crystal structures. c) TEM image of the 14 nm polymer coated nanoparticles with high magnification image showing the dark contrast zero valent iron core and light contrast iron oxide shell. d) SAED of the nanoparticles in (c) indexed to zero valent iron and iron oxide (magnetite or maghemite) crystal structures.

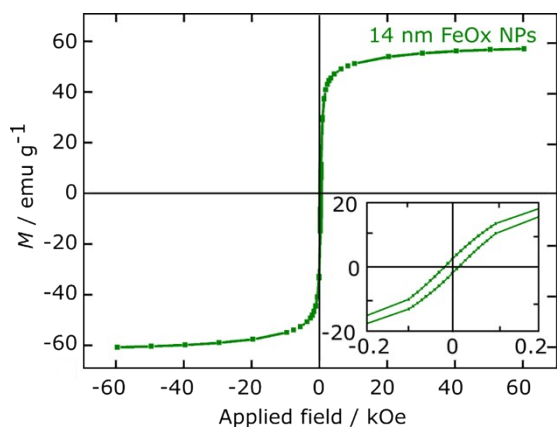


**Figure S5:** Hysteresis loop of 14 nm iron oxide nanoparticles at room temperature.  $M_{\text{sat}} = 58 \text{ emu g}^{-1}$ , remnant magnetization =  $1 \text{ emu g}^{-1}$ , coercivity = 2 Oe.

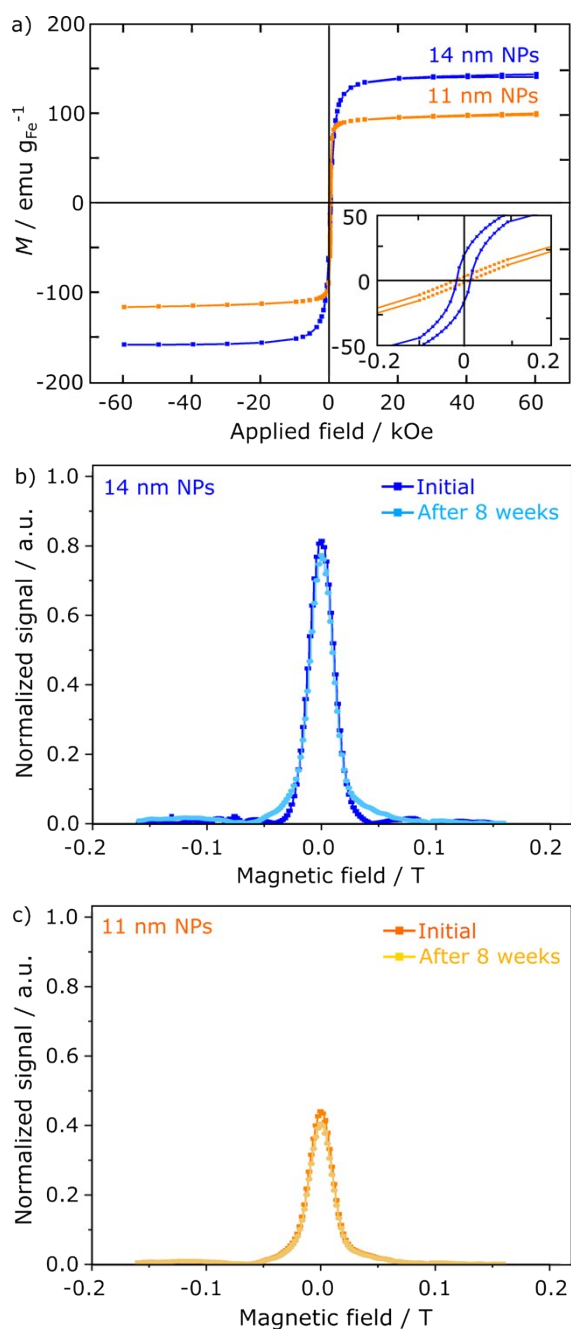


**Figure S6:** Stability of magnetic performance. a) Hysteresis loops of polymer coated 14 nm (blue) and 11 nm (yellow) nanoparticles after 8 weeks in aqueous media. b) MPI point spread functions for 0.7  $\mu\text{g}$  polymer coated 14 nm nanoparticles before (dark) and after (light) 8 weeks in aqueous media. c) MPI point spread functions for 0.7  $\mu\text{g}$  polymer coated 11 nm nanoparticles before (dark) and after (light) 8 weeks in aqueous media.

## References

- 1 D. A. J. Herman, S. Cheong-Tilley, A. J. McGrath, B. F. P. McVey, M. Lein and R. D. Tilley, *Nanoscale*, 2015, **7**, 5951–5954.
- 2 A. J. McGrath, S. Cheong, A. M. Henning, J. J. Gooding and R. D. Tilley, *Chem. Commun.*, 2017, **53**, 11548–11551.
- 3 R. Qiao, L. Esser, C. Fu, C. Zhang, J. Hu, P. Ramírez-Arcía, Y. Li, J. F. Quinn, M. R. Whittaker, A. K. Whittaker and T. P. Davis, *Biomacromolecules*, 2018, **19**, 4423–4429.